

## Characterization and Expression Analysis of *HbC3H66*: Implications for Transcriptional Regulation in Rubber Biosynthesis and Abiotic Stress Responses in *Hevea brasiliensis*

Wanphen Buakong<sup>1</sup>, Pluang Suwanmanee<sup>2</sup>, Thanika Vasinayanuwatana<sup>3</sup>, Kedsirin Ruttajorn<sup>4,\*</sup>, Kasem Assawatreratanakul<sup>5</sup> and John Espie Leake<sup>6</sup>

<sup>1</sup>International College, Thaksin University, Songkhla 90000, Thailand

<sup>2</sup>Institute of Community Operation and Life-long learning, Thaksin University, Songkhla 90000, Thailand

<sup>3</sup>Department of Teaching Science, Mathematics, Faculty of Education, Thaksin University, Songkhla 90000, Thailand

<sup>4</sup>Department of Biology, Faculty of Science, Thaksin University, Phatthalung 93110, Thailand

<sup>5</sup>International College, Thaksin University, Songkhla 90000, Thailand

<sup>6</sup>School of Economics and Public Policy, Faculty of the Professions, The University of Adelaide, Adelaide 5005, Australia

(\*Corresponding author's e-mail: kedsirin@tsu.ac.th)

Received: 7 March 2023, Revised: 22 April 2023, Accepted: 8 June 2023, Published: 15 September 2023

### Abstract

CCCH-type zinc-finger protein (ZnF\_CCCH) family is one of the most important transcription factors (TFs) linked to various biotic and abiotic stressors and physiological and developmental processes in plants. This study aims to clone and characterise the latex gene expression patterns, evolution and characteristics of the *Hevea brasiliensis* ZnF\_CCCH domain-containing protein 66 (*HbC3H66*) gene. These results showed that the open reading frame (ORF) of the *HbC3H66* gene was 2,106 bp, encoding 701 aa and the calculated molecular weight of the encoded protein was 76.52 kDa. The N-terminal region of *HbC3H66* contains 2 ANK repeats in, PFK\_2/FBPase-2 and 2 type zinc finger motifs. Phylogenetic analysis showed that the C3H66 amino acid from *Hevea* and other plant C3H66 were clustered into 1 group and could be used for evolutionary analysis. Semi-quantitative RT-PCR (sqRT-PCR) revealed that the *HbC3H66* mRNA was abundance in high-yielding *Hevea* clones (RRIT251 and RRIM600) and treatment with 2.5 % of ethephon (Eth) induced *HbC3H66* mRNA expression in the latex of 15 years old *Hevea* trees. The *HbC3H66* gene was induced by water deficit and 0.5 M NaCl in the latex of 3-month-old *Hevea*. In conclusion, the *HbC3H66* protein may play a role in DNA-binding transcriptional regulation in NR pathways. Which would provide a theoretical basis for understanding the evolution and functions of the *Hevea C3H66* gene in rubber biosynthesis.

**Keywords:** CCCH-type zinc finger protein, *Hevea brasiliensis*, Water deficit, Transcription factor, Ethylene, Drought stress, Salt stress

### Introduction

*Hevea brasiliensis* is an important economic and industrial crop on natural rubber-producing plants. Natural rubber (NR) which the constituent of monomer isopentenyl pyrophosphate (IPP) is synthesized from the mevalonate (MVA) pathways and possibly also from the 2-C-methyl-D-erythritol-4-phosphate (MEP) pathway in plants, multiple feedback mechanisms regulate both the MVA and MEP pathways [1]. The cytosolic mevalonate (MVA) pathway in *H. brasiliensis* latex is the conventionally accepted pathway which provides IPP for *cis*-1,4-polyisoprene (NR) biosynthesis. However, the plastidic MEP pathway may be an alternative source of IPP since its more recent discovery in plants. The presence of numerous rubber particles in the cytoplasm of laticifer cells, commonly known as latex, was an expression of the quantity and type of several genes involved in the stress response and biosynthesis of secondary metabolites. These genes all contribute to disease resistance and environmental adaptability [2]. In rubber production, the bark of *Hevea* trees is tapped for latex, usually every 3 days. This method induced stress on rubber trees, and they protected themselves by synthesizing rubber molecules. The NR biosynthesis pathways are now fully understood while the positive feedback control of rubber biosynthesis is poorly understood. However, the regulation mechanism of the NR biosynthesis gene in the rubber tree has not yet been thoroughly investigated. Some transcription factors (TFs) participate in the activated genes responsible for NR

biosynthesis in *Hevea* trees. For example, 2 TFs, including *Hb\_bHLH1* and *Hb\_bHLH2* gene, upregulate the expression of *HbREF3* and *HbSRPP1* gene [3]. Therefore, the *HbCZF1* gene upregulates the expression of *HMGR1* gene [4]. *HbHMGR2*, *HbHMGS2*, *HbCPT6*, *HbCPT8* and *HbSRPP2* gene significantly increase when upregulated by *HbTGAI* gene under salicylic acid [5]. As a result, TFs are critically important to the process of NR biosynthesis.

CCCH-type zinc-finger proteins (ZnF\_CCCH) transcription factors (TFs) play important roles in plant growth and stress tolerance. It enables plants to endure adverse environmental conditions like low temperatures, salinity, drought and flooding [6]. Zinc finger proteins (ZnF) with the motif of 3 cysteine (C-C-C) and histidine (H) residues are produced by the gene belonging to the ZnF\_CCCH family [7]. It forms proteins known for their finger-like structure and ability to bind  $Zn^{2+}$ . Classifying these proteins as tandem ZnF\_CCCH (TZF) or non-TZF proteins depends on how many and where these CCCH motifs are present. Tandem motifs are absent from non-TZF proteins, whereas TZF proteins contain tandem ZnF\_CCCH motifs [8]. The non-TZF and TZF genes are essential for various biological activities, including the development of biotic and abiotic stresses [9]. An arginine-rich (RR) region is found in front of the TZF motif (RR-TZF) in many plants. Overall, there are 2 categories of plant RR-TZF proteins: ANK-RR-TZF, which also includes the ANK (Ankyrin) domain and RR-TZF, which has the RR and TZF domains. The plant ANK-RR-TZF domain has mechanisms like that of animals, and wherein TZF is responsible for RNA targeting and transcriptional regulation in response to stress. These proteins contribute to drought tolerance [10]. In addition, the mechanism governing the ZnF\_CCCH protein is rarely reported in *Hevea* trees, and the regulation of expressions remains unclear.

It has been reported that each *Hevea* clone can withstand drought differently. Among the clones evaluated in the field conditions clone, RRIM600 exhibits better growth and yield [11]. Moreover, Tapping Panel Dryness (TPD), a physiological disease, is becoming more common as domestic farmers use high-yielding rapid clones and intensive harvesting systems, which causes an ongoing decline in rubber production. TPD causes an estimated 12 - 20 % loss in rubber output, which can rise due to climate change. Environmental and harvesting stresses can cause oxidative stress and TPD induction in laticifers [12].

The *zinc finger CCCH domain-containing protein 66 (HbC3H66)* gene in *Hevea* trees needs more research into the controlled mechanisms of rubber production and stress tolerance. The protein is one of the subgroups of the ZnF\_CCCH protein family. The mechanism of this gene has not been previously uncharacterized in rubber trees; therefore, the current study focuses on recent advances in deciphering the nucleotide sequences, structures, functions and classifications of the *HbC3H66* gene, as well as its roles in abiotic stress (water deficit and salinity) and ethylene treatment responses. Once the functional group is known and the expression of this gene exhibits a positive correlation with yielding and abiotic stress, we can use the relationship to identify high-yielding and drought-tolerant *Hevea* clones. Therefore, this research emphasizes the zinc finger CCCH gene since the high-yielding *Hevea* clone is sensitive to TPD symptoms due to drought stress.

## Materials and methods

### Plant material and poly (A)<sup>+</sup> mRNA isolation

A plantation ran by the Department of Basic Science and Mathematics, Faculty of Science, Thaksin University, Songkhla, Thailand, was used to cultivate 3-month *Hevea* clone RRIT251 seedlings. The rubber trees were grown in a greenhouse with a natural photoperiod of approximately 12/12 h light/dark cycle; with 10 replicated each treatment. During this time, they were subjected to a period of water deficit (1, 2, 4, 5, 6 and 8 days, respectively). The control treatment was provided water every day. For the salt stress treatment, 0.5 M NaCl solution was treated with seedling *Hevea* trees (0.5, 3, 6, 12 and 24 h, respectively), water was used to control treatment.

The 15 years old of high-yielding (RRIT251, RRIM600) and low-yielding (KRS138, BPM3) *Hevea* clones were grown in the Rubber Authority of Thailand, Surat Thani province, Thailand, were tapped every second day. The 15 years old, high yielding *Hevea* clones (RRIT251) grown in an experimental field in Thamod subdistrict, Phatthalung province, Thailand, were used to assess the effects of ethylene treatment. 2.5 % of ethephon (Eth) (2-chloroethane phosphonic acid) was applied to the tapping panel of the tree bark. A RRIT251 rubber tree without the Eth treatment was used as a control. Fresh latex was collected from trees 1 day before the treatment and once every 3 days after the treatment, and all this for 5 times with 5 replicated each treatment. Samples of fresh latex collected from rubber trees were kept on ice before RNA was isolated. Fresh latex was dried at 70 °C in an oven for 2 days for constant weight.

According to Suwanmanee *et al.* [13], the total RNA was extracted from the latex of *Hevea* trees using the phenol-chloroform method. The poly (A)<sup>+</sup> was isolated from total RNA using the Oligotex mRNA

Mini Kit (QIAGEN, Maryland, USA), in accordance with the manufacturer's instructions. Agarose electrophoresis and a UV-visible spectrophotometer were used to determine the quality and concentration of the RNA samples.

#### Isolation and analysis of the full-length cDNA

Previously, the *zinc finger CCCH domain-containing protein 66 (HbC3H66)* gene has been isolated in the latex of high-yielding *Hevea* clones (RRIT251) using a cDNA-AFLP technique [14]. The full-length cDNA was examined using the RACE method using 242 bp of the *HbC3H66* gene. The poly (A)<sup>+</sup> mRNA was used as a template for performing 3'- and 5'-RACE reactions based on the cDNA partial sequence of *HbC3H66*. 5'-end and 3'-end cDNA fragments were generated from mRNA using SMARTer™ RACE cDNA amplification kit (Takara Bio, USA), following the manufacturer's protocol using Universal Primer Mix (UPM) and gene-specific primers (5'-GSP1 or 3'-GSP2). Nested 5'-RACE PCR was carried out utilizing UPM as a forward primer and one of 3 nested gene-specific reverse primers (NGSP1, NGSP2 and NGSP3). The *HbC3H66* cDNA fragment was used in a QIAquick gel extraction kit (QIAGEN, Germany) and then ligated into the pGEM-T-Easy vector (Promega Corporation, USA). It was subsequently converted into competent *E. coli* DH5 $\alpha$  cells to establish the nucleotide arrangement.

#### DNA sequencing and computer analysis

The sequence of the DNA fragments comprising the *HbC3H66* arrangement was used for the dideoxy chain termination method kit (ABI prism377 DNA sequence, Thermo Fisher Scientific, USA). A BLAST analysis was performed to compare the DNA and predict amino acid sequences using the non-redundant database employing programs provided by the National Centre of Biotechnology Information (NCBI, USA)'s database. The physicochemical of *HbC3H66* was computed using the ExPASy ProtParam tool [15]. All the amino acid sequences of C3H66 in the plants were verified. We exploited the Clustal W algorithm in the BioEdit program (version 7.2.5) to align the amino acid sequence of *HbC3H66* from latex and other plants of C3H66 [16]. The coding region of the nucleotide sequences were determined using the Open Reading Frame (ORF) Finder tool (<https://www.ncbi.nlm.nih.gov/orffinder/>). Phylogenetic reconstruction and evolutionary distance were computed using MEGA11 software, with default parameters of 1,000 bootstrap replicates and the maximum likelihood technique [17]. The *HbC3H66* gene's translated sequences were examined using the conserved domain database with the SMART tool [18], and NCBI (<https://www.ncbi.nlm.nih.gov/Structure/lexington/lexington.cgi>). Using TMHMM, we analysed the *HbC3H66* protein's predicted transmembrane structure (<http://www.cbs.dtu.dk/services/TMHMM-2.0/>). We created the logos for the CCCH zinc finger motifs using Online WebLogo software [19]. We built the domain information website utilizing IBS 1.0.3 software [20]. We evaluated nuclear localization signal (NLS) using the cNLS mapper [21].

#### Protein structure and modelling

I-TASSER was used to create a 3D structural *HbC3H66* protein using the Protein Data Bank (PDB) [22]. PyMOL can enable in displaying the generated 3D structure [23]. PROCHECK and Mol-Probity programs were employed to assess the model's stereochemical quality by quantifying the residues in the allowed zones of the Ramachandran plot [24].

#### Semi-quantitative RT-PCR (sqRT-PCR) evaluation

Total RNA from the latex of *Hevea* trees was used to analyze the function of this gene using the sqRT-PCR technique. AMV reverse transcriptase (Promega, Madison, WI) was used to reverse-transcribe 2  $\mu$ g of the total RNA from each sample according to the manufacturer's instructions. The expression frameworks of *HbC3H66* gene were assessed using sqRT-PCR with the gene-specific primer of *HbC3H66*-F-5'- CCGGGGATCAACGAAGTAC-3' and *HbC3H66*-R-5'-CCGAGGCCTTACAATAAAC- 3'. The PCR was conducted on 25 cycles at 94 °C for 30 s, 56 °C for 30 s and 72 °C for 2 min. The 18S rRNA gene was used as an internal reference 18SF 5'- CAAAGCAAAGCCTACGCTCTG -3' and 18SR 5'-CGCTCCACCAACTAAGAACG -3' with the cycling parameter, and then 15 cycles at 94 °C for 30 s, 58 °C for 30 s and 72 °C for 2 min. The relative expression levels were calculated using Quantity One analysis software (Bio-Rad, Hercules, CA, USA).

#### Statistical analysis

By performing a 1-way analysis of variance (ANOVA) with SPSS 21, the statistical significance was evaluated. A significant difference was defined as one with a *p*-value of 0.05 or above, and an extreme difference as one with a *p*-value of 0.01. Every piece of data was displayed as mean  $\pm$  SE.

## Results and discussion

### Isolation and sequence analysis of the zinc finger CCCH domain-containing protein 66 (*HbC3H66*) gene from *H. brasiliensis*

The cDNA of *HbC3H66* contained 2,596 bp, and an ORF of 2,106 bp encoded a protein having 701 amino acid residues with ATG as the initiation codon. The 5'-untranslated region (UTR) and 3'-UTR were 194 and 299 bp, respectively, with a polyadenylation (poly A) tail. The molecular weight, theoretical pI and aliphatic index of *HbC3H66* were 76,522.03 Da, 5.60 and 74.42, respectively. Its stability index and GRAVY were 55.67 and  $-0.372$ , respectively. Assuming that all pairs of Cys residues form cystine, the EC will be 75,495. Assuming that all Cys residues are reduced, the EC will be 74,370. The half-life (h) is 30 h. There were 66 positively charged residues (Arg + Lys) and 81 negatively charged residues (Asp + Glu) in total.

The predicted transmembrane domain of the deduced *HbC3H66* protein showed that there was extracellular protein (region 1 - 701 aa). This sequence was registered in the GenBank database (accession number MN866526). *HbC3H66* encoded putative CCCH (C-X<sub>7</sub>-C-X<sub>5</sub>-C-X<sub>3</sub>-H)-type zinc finger proteins, which included 2 conserved tandem ZnF\_CCCH between 74 - 104 and 109 - 141 aa. The functional sites including conserved ANK repeat and 6-phosphofructo-2-kinase/fructose-2,6-biphosphatase (Pfk\_2/FBPase-2) binding sites in the N-terminal regions were predicted in the deduced *HbC3H66* protein (Figure 1(A)). Sequence logos for common C3H66 zinc finger motifs of plants, C-X<sub>5</sub>-H-X<sub>4</sub>-C-X<sub>3</sub>-H (arginine-rich region; RR), C-X<sub>7</sub>-C-X<sub>5</sub>-C-X<sub>3</sub>-H motif and C-X<sub>5</sub>-C-X<sub>4</sub>-C-X<sub>3</sub>-H (TZF motif) are shown in Figure 1(B). These results shown this gene are TZF protein and the type of ANK-RR-TZF domain. *HbC3H66* is also a member of subfamily IX of the zinc finger CCCH family, since these subfamilies consist of C-X<sub>7-8</sub>-C-X<sub>5</sub>-C-X<sub>3</sub>-H and C-X<sub>5</sub>-C-X<sub>5</sub>-C-X<sub>3</sub>-H disjointed using 16 amino acids and a preserved 50 amino acid concentration upstream of the CCCH motif [9].

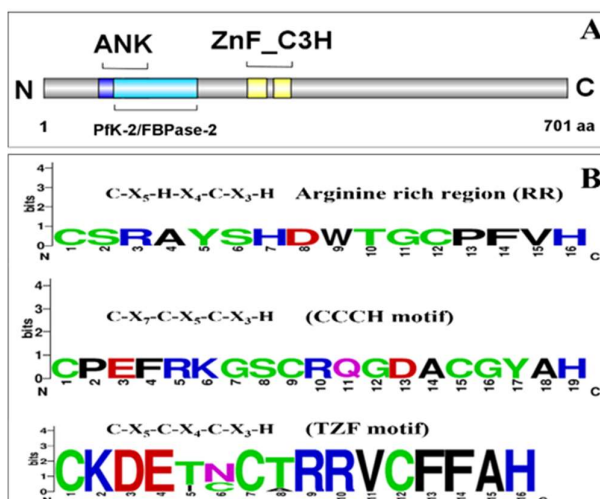


**Figure 1** Conserved domain of ZnF\_CCCH proteins in *H. brasiliensis* contained 2 CCCH motifs. SMART and NCBI (<http://www.ncbi.nlm.nih.gov/Structure/cdd/wrpsb.cgi>) identified the conserved domain of CCCH proteins, and the expect Value was set to 5. The domains information site was developed using IBS 1.0.3. A) ANK, ankyrin repeat domain; ZnF\_C3H, CCCH-type zinc finger motif; and Pfk 2/FBPase-2, 6-phosphofructo-2-kinase/fructose-2,6-biphosphatase and B) sequence logos for prevalent plant C3H66 zinc finger motifs.

### Multiple alignments and phylogenetic analysis of *HbC3H66*

Multiple alignments were conducted to analyze the homology of deduced *HbC3H66* protein with the homology of ZnF\_CCCH containing domain protein 66 (C3H66) *Manihot esculenta* (XP\_021604126.1), *Ricinus communis* (XP\_002525655.1), *Salix suchowensis* (KAS5238360.1), *Populus trichocarpa* (XP\_002299802.3), *Juglans regia* (XP\_018835448.1), *Theobroma cacao* (XP\_007016084.2), *Hebececnema umbratica* (XP\_039041436.1) and *Durio zibethinus* (XP\_022755897.1) with 84.9, 80.8, 77.0, 76.3, 74.3, 72.1, 71.9 and 70.3 %, respectively. The results showed that amino acid sequences were highly conserved with C3H66, which exhibited low homology with *D. zibethinus* and *J. regia*. In plants, the C3H66 had 2 tandems of CCCH-type zinc finger proteins. All of them had 2 tandem ankyrin repeats (Figure 2(A)). But

these protein in *H. brasiliensis*, *M. esculenta*, *P. alba* and *P. trichocarpa* is extra addition of PFK-2/FBPase-2 in the conserved domain. The function of members of this protein family is unknown in *Hevea* trees. We used a program from Liu *et al.* [20], to detected NLS in *Hbc3H66* protein, and found all members contained a putative NLS sequence, indicating that they may be nucleocytoplasmic shutting proteins involved in signal transduction (**Figure 2(B)**). From the previous study, ZnF\_CCCH, including 2 ANK repeat domains and 2 TZF motifs in the N-terminal, were regulated in the salt and drought response in plants [25]. Consequently, this protein acts as a *cis*-element in the nucleus that binds DNA for transcription factors [26]. When responding to stress, some ZnF\_CCCH attach primarily to AU-rich regions of the target mRNA [27]. Moreover, the *Hbc3H66* protein excludes any known RNA binding domain, such as the RNA recognition motif (RRM) or K homolog domain [28].

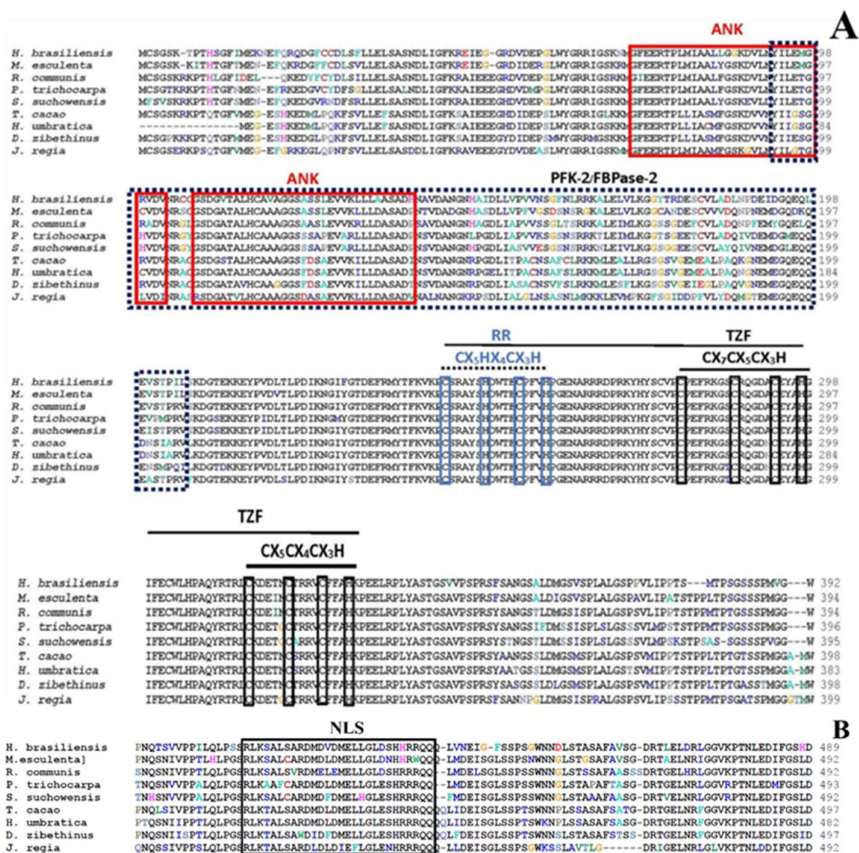


**Figure 2** Multiple alignment of the ZnF\_CCCH from various species. *Hevea brasiliensis* (QQL94539.1), *Manihot esculenta* (XP\_021604126.1), *Ricinus communis* (XP\_002525655.1), *Salix suchowensis* (KAS5238360.1), *Populus trichocarpa* (XP\_002299802.3), *Juglans regia* (XP\_018835448.1), *Theobroma cacao* (XP\_007016084.2), *Hebecnema umbratica* (XP\_039041436.1), and *Durio zibethinus* (XP\_022755897.1). A) The CCCH-type zinc finger motifs are lined above, the ANK domains are displayed in boxes, and PFK-2/FBPase-2 is in the dotted boxes and B) amino acid sequence alignment of putative NLS sequence in plant C3H66 (B).

This study generated a phylogenetic tree to compare the phylogenetic relationships between *Hbc3H66*, its paralog and orthologs. Phylogenetic analysis revealed that the C3H66 protein from *H. brasiliensis* and other plants C3H66 generated a branch (**Figure 3**). C3H66 proteins with the PFK-2/FBPase-2 domain is phylogenetic and belong to the Malpighiales order. The current model processes that PFK-2/FBPase-2 coordinates sucrose synthesis with starch formation and photosynthetic activity [29].

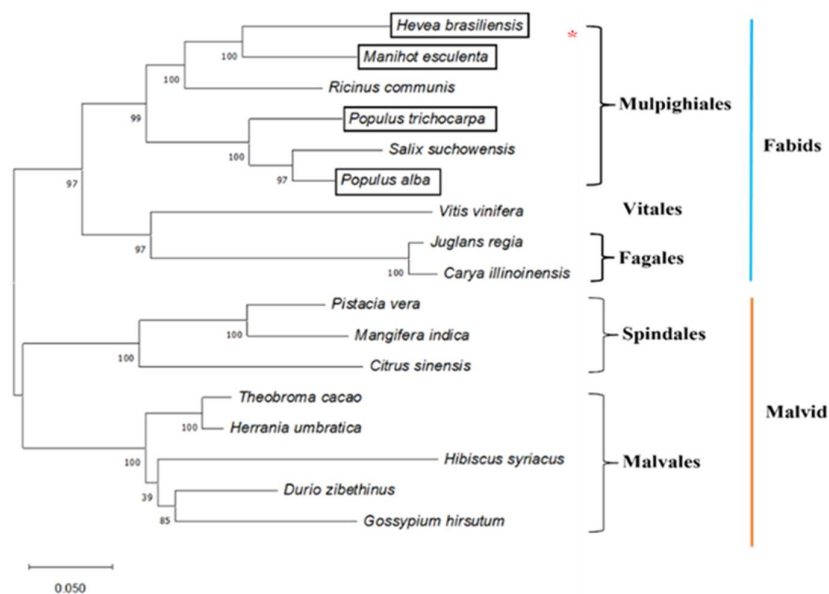


**Figure 3** Phylogenetic analysis of plants C3H66 protein *H. brasiliensis* was marked with box and the star, and the taxonomies in the order level was indicated on the right. The boxes are shown Pfk\_2/FBPase-2 in the conserved domain.

#### Model validation

I-TASSER was employed in comparative modelling to forecast the 3D structure of *HbC3H66* [21]. The results showed 23 % identity to the structure of Ankyrin repeat protein (ANK-N5C) synthetic construct (PDB ID: 4060 chain A) as a DNA-binding transcription activator [30] and 6 % to the monomer of TRAPP11 (open) in *Saccharomyces cerevisiae* (PDB ID: 7E2C chain A) as a transport protein particle [31]. On the N-terminal side of the protein, ligand binding sites are located between amino acids 58 to 361 (**Figure 4**). We compare structure using a TNP01\_HUMAN Uniprot ID Q92973. This protein, function in nuclear import as nuclear transport receptor. Serves as receptor for nuclear localization signals (NLS) in cargo substrates [32]. *HbC3H66*, a member of the ANK-RR-TZF subfamily, may be a nucleocytoplasmic shuttling protein involved in signal transduction, according to 3D structural modelling (**Figure 4**) [33].

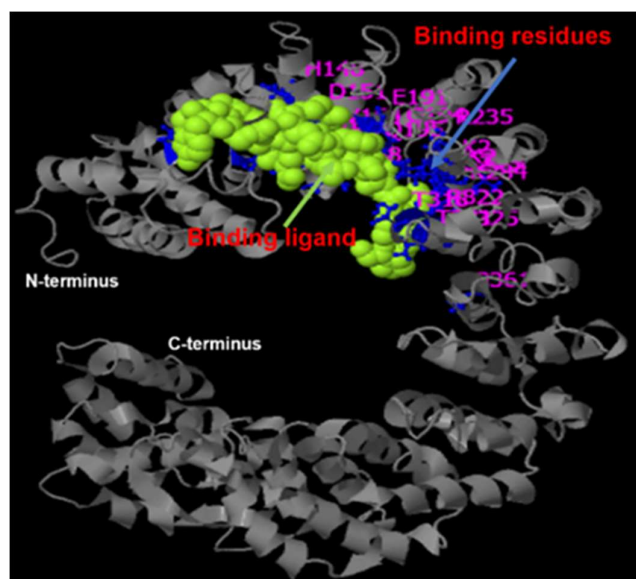


**Figure 4** The prediction 3D structure models of the *HbC3H66*, and the ligand binding sites.

### *HbC3H66* mRNA expression abundance in high-yielding *Hevea* clone

Using sqRT-PCR, we analysed the *HbC3H66* transcript levels in different *Hevea* clones. The result showed that high-yielding *Hevea* clones (RRIT251 and RRIM600) (**Figure 5(A)**) have high levels of *HbC3H66* expression, while low-yielding *Hevea* clones (BPM3 and KRS138) (**Figure 5(B)**) exhibited lower levels of expression. The RRIT251 clone had the highest concentration of dried rubber, while the KRS138 clone had the lowest (**Figure 5(C)**). In the laticifer cells of rubber trees, a transcriptional factor known as *HbC3H66* gene is active and integrated into the mediator of rubber biosynthesis. According to the experimental findings, the RRIM600 *Hevea* clone displayed the highest amount of *HbC3H66* expression. This expression level did not differ significantly from the expression levels in low-yielding KRS138 and BPM3 (**Figure 5**). These findings support the systematic comparison and analysis of 2 high rubber yield clones, RRIM600 and RY7-20-59, and imply that RY 7-20-59's higher natural rubber production is probably due to a greater overall IPP availability and better IPP distribution for rubber biosynthesis [34,35]. This is in line with the fact that the clones RRIM600 and GT1 produce more and can withstand drought circumstances better because their leaves have higher vacuolar invertase (VINN) activity, which ensures more significant vascular reducing sugars (RS) accumulations [36].

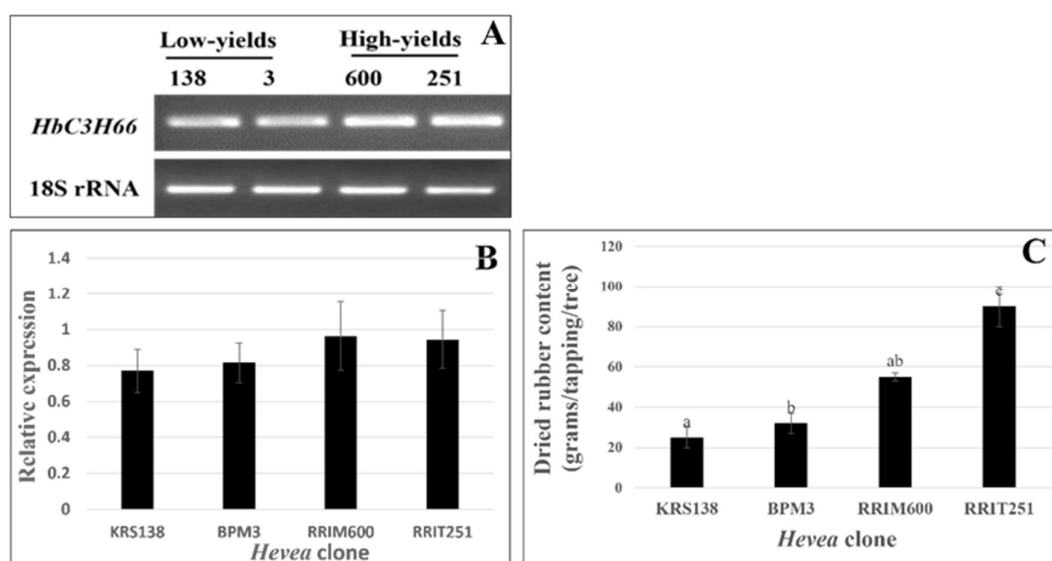


**Figure 5** *HbC3H66* mRNA expression determined in latex of various *Hevea* clone A) Semi-quantitative RT-PCR analysis of *HbC3H66* transcripts of *Hevea* clone, B) Relative expression of *HbC3H66* mRNA of *Hevea* clone and C) The dried rubber contents of *Hevea* clone. Significant difference at  $p < 0.05$  is indicated by letters above the bars ( $n = 10$  replicates).

### Ethylene induced *HbC3H66* mRNA expression

At *Hevea* clone RRIT251, Ethepon (Eth) was applied at a rate of 2.5 % to the tapping panel of the bark. Each of the 5 duplicates of each Eth treatment received 1 treatment. After the Eth treatment, samples of both the untreated control trees and the treated test trees were collected 24 h later. The expression pattern of *HbC3H66* gene in the latex of 15-years old *Hevea* trees was affected by Eth treated. The highest level of *HbC3H66* expression was significantly after trees treated Eth in 3 days ( $p < 0.05$ ) (**Figures 6(A) - 6(B)**). The dried rubber content was analyzed. The results shown in *Hevea* treated trees was abundance of dried rubber content with no statistically significant differences between the treatments (**Figure 6(C)**). Ethylene was differentially perceived and transduction in latex. In contrast to the control, the latex of *Hevea* trees treated with Eth had a greater relative transcript abundance of *HbC3H66* (**Figure 6**). The *HbC3H66* gene had a higher transcript abundance in latex for 3 days after Eth treatment and tapped tree. They corresponded to the transcriptomes analysis of *H. brasiliensis* PR107 and were treated with Eth. It revealed the upregulation of the key genes involved in water transfer, sucrose allocation, glycolysis and C3 carbon fixation. These genes are upregulated in the glycolytic pathway and Calvin cycles. Instead, rubber biosynthesis might be responsible for ethylene-induced latex production in rubber trees [37].

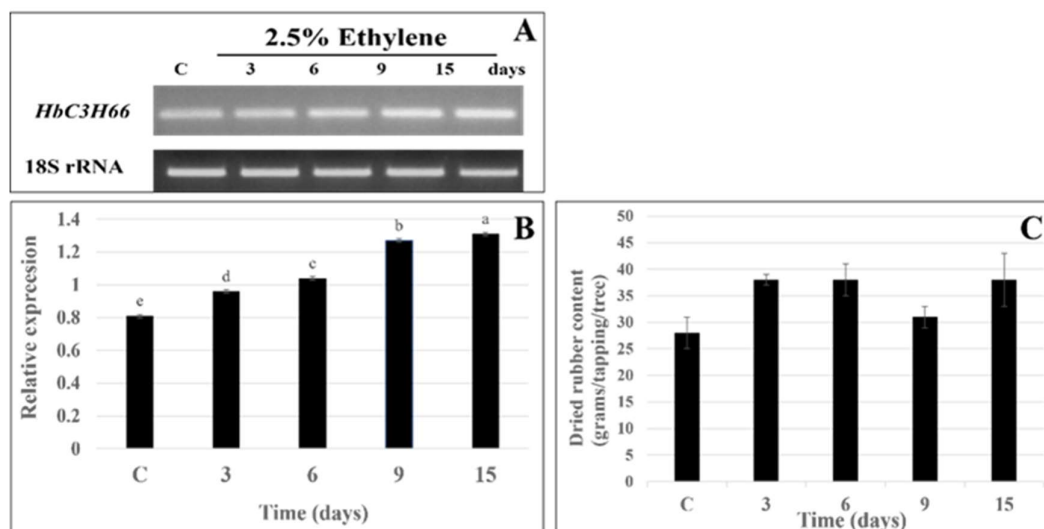


**Figure 6** *HbC3H66* mRNA expression determined in latex of 15-year-old RRIT251 *Hevea* clone. A) Semi-quantitative RT-PCR analysis of *HbC3H66* transcripts after Eth treatment, B) relative expression of *HbC3H66* mRNA after Eth treatment and C) The dried rubber contents of Eth treated *Hevea* trees. Significant difference at  $p < 0.05$  is indicated by letters above the bars (n = 5 replicates).

#### ***HbC3H66* transcriptionally responsive to drought and salt stress**

To determine if *HbC3H66* responds to abiotic stressors, this study examined its relative expression pattern under a variety of situations. *HbC3H66* was highly inducible by NaCl treatment as its expression level increased by 1.19- and 1.18- fold after 0.5 and 6 h of salt was applied, respectively (**Figure 7**). *HbC3H66* was also responsive to water deficit-induced drought stress, with a 1.5-fold up-regulated expression after 2 days of treatment (**Figure 8**). The expression of *HbC3H66* was responsive to abiotic stress. The stress responses were used to create a water deficit and salt stress to induce the expression of the *HbC3H66* mRNA in the latex of the trees (**Figures 7 and 8**). *HbC3H66* was transcriptional responsive to water deficit and salt. This was the same as the gene of *BnC3H66* from *Brassica*, which responds to water deficit (PEG) and ABA [38]. The polypeptide Pfk-2/FBPase-2 that *HbC3H66*'s N-terminal domains have the most in common with mammalian PFK-2s contains several tandem repeat ANK motifs. Therefore, it known to mediate protein-protein interactions and more specialised receptors for sensing abiotic challenges, such as salt, osmotic and low-temperature stresses, helps plants respond to various environmental stresses [39]. According to the results from Banzai *et al.* [40], during a drought, plants are stressed in which many plants accumulate soluble sugars, which are likely to be osmotic to prevent further desiccation. That control activities of Pfk-2/FBPase-2 that the dramatic increase in leaf tissue during drought or osmotic stress. By controlling the production of sucrose, Banzai *et al.* [41], postulate that these proteins may be crucial in an osmotic adaptation.

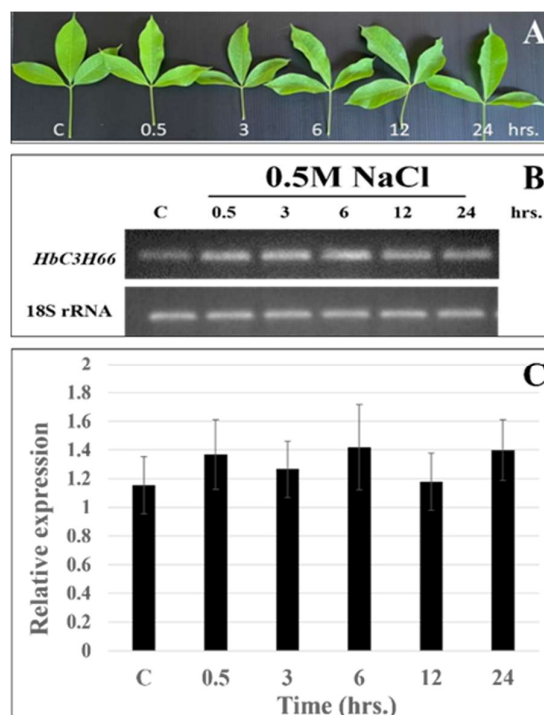


**Figure 7** *HbC3H66* mRNA expression determined in latex of seedling RRIT251 *Hevea* clone. A) Leaves of seedling *Hevea* tree was treated with NaCl, B) semi-quantitative RT-PCR analysis of *HbC3H66* transcripts after NaCl treatment and C) Relative expression of *HbC3H66* mRNA after NaCl treatment. Substantial difference is indicated by letters above the bars when  $p < 0.05$  ( $n = 10$  replicates).

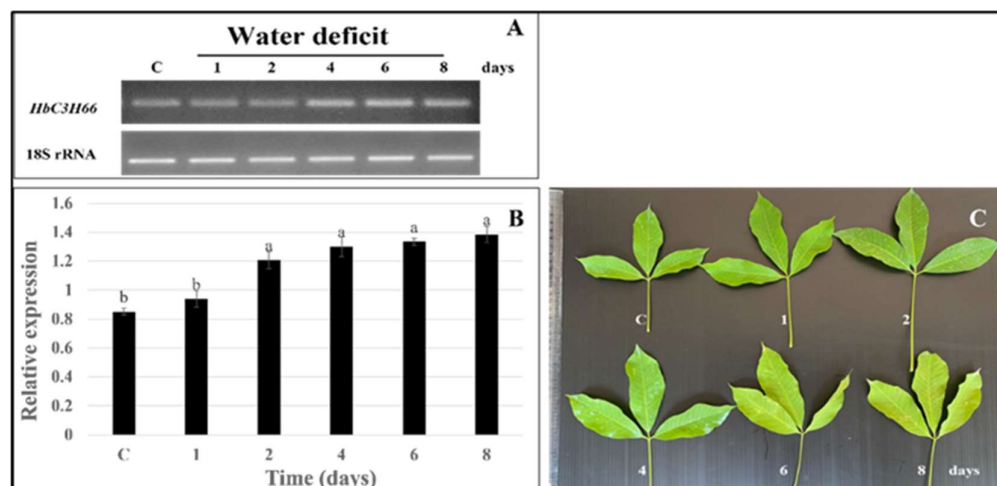


**Figure 8** *HbC3H66* mRNA expression determined in latex of seedling RRIT251 *Hevea* clone. A) Semi-quantitative RT-PCR analysis of *HbC3H66* transcripts after water deficit treatment, B) relative expression of *HbC3H66* mRNA after not water deficit treatment and C) leaves of seedling *Hevea* tree was treated with a water deficit. Significant difference at  $p < 0.05$  is indicated by letters above the bars ( $n = 10$  replicates).

According to Guo and Chong [42], *Arabidopsis thaliana* and *Oryza sativa* rapidly respond to specific abiotic stress based on which type of sensor is stimulated. As this determines which series of responses is activated upon sensing the stress signal, plants produce second messengers (such as a  $\text{Ca}^{2+}$  pulse) in the cytoplasm, which act on a series of downstream genes, including CCCH zinc-finger protein genes [6]. The changes in  $\text{Ca}^{2+}$  concentration is sense by several  $\text{Ca}^{2+}$  sensors or  $\text{Ca}^{2+}$ -binding proteins [43]. In line with

*H. brasiliensis*, previously identified the putative transcription factors, including MYB, zinc finger, bHLH, bZIP, PHD finger and NAC domain-containing family members, which paved the way to discover the regulatory mechanisms of natural rubber metabolism and accelerated our understanding of the gene regulator network in rubber laticifer [44]. The results suggest that the *HbC3H66* protein may play a role in transcriptional regulation via protein-protein interaction in rubber biosynthesis.

### Conclusions

In conclusion, this research leads to understanding the role of *HbC3H66* in rubber trees. *H. brasiliensis* zinc finger CCCH domain-containing protein 66 (*HbC3H66*) gene was clone and characteristics. The *HbC3H66* contains 2 ANK repeat in, Pfk<sub>2</sub>/FBPase-2 and 2 type zinc finger motifs. Semi-quantitative RT-PCR revealed that the *HbC3H66* mRNA was abundance in high-yielding *Hevea* clones (RRIT251 and RRIM600), treatment with ethephon induced *HbC3H66* mRNA expression in the latex of 15-years old *Hevea* trees. Water deficit and NaCl induced this gene in the latex of 3-month-old seedling *Hevea* trees. The results show that the *HbC3H66* protein may play a role in DNA-binding transcriptional regulation in NR pathways. An in-depth study on the mechanism of gene linkage in rubber molecule synthesis, drought tolerance and TPD formation, which are forwarded to each other as a system, should be further conducted.

### Acknowledgements

The author would like to offer particular thanks to Rubber Authority of Thailand, Surat Thani Province, Thailand for the high and low yielding *Hevea* clone materials. This research was supported by the research council of Thailand (NRCT) (grant no. 2553A10501003) and Funded by the Personnel Development Fund of Thaksin University, Songkhla province, Thailand. The authors declare that there is no conflict of interest among authors as well as any other individual and organization.

### References

- [1] S Cherian, SB Ryu and K Cornish. Natural rubber biosynthesis in plants, the rubber transferase complex, and metabolic engineering progress and prospects. *Plant Biotechnol. J.* 2019; **17**, 2041-61.
- [2] X Men, F Wang, GQ Chen, HB Zhang and M Xian. Biosynthesis of natural rubber: Current state and perspectives. *Int. J. Mol. Sci.* 2019; **20**, 50.
- [3] T Yamaguchi, Y Kurihara, Y Makita, EO Kurihara, A Kageyama, E Osada, S Shimad, H Tsuchida, H Shimada and M Matsui. Regulatory potential of bHLH-type transcription factors on the road to rubber biosynthesis in *Hevea brasiliensis*. *Plants* 2020; **674**, 2-13.
- [4] D Guo, HY Yi, HL Li, C Liu, ZP Yang and QS Peng. Molecular characterization of *HbCZF1*, a *Hevea brasiliensis* CCCH-type zinc finger protein that regulates *hmg1*. *Plant Cell Rep.* 2015; **34**, 1569-78.
- [5] D Guo, HL Li, JH Zhu, Y Wang and SQ Peng. *HbTGA1*, a TGA transcription factor from *Hevea brasiliensis*, regulates the expression of multiple natural rubber biosynthesis genes. *Front. Plant Sci.* 2022; **13**, 909098.
- [6] G Han, Z Qiao, Y Li, C Wang and B Wang. The roles of CCCH zinc-finger proteins in plant abiotic stress tolerance. *Int. J. Mol. Sci.* 2021; **22**, 8327.
- [7] PJ Blackshear. Tristetraprolin and other CCCH tandem zinc finger proteins in the regulation of mRNA turnover. *Biochem. Soc. Trans.* 2002; **30**, 945-52.
- [8] HY Seok, H Bae, T Kim, MMM Syed, LV Nguyen, SY Lee and YH Moo. Non-TZF protein AtC3H59/ZFWD3 is involved in seed germination, seedling development, and seed development, interacting with PPPDE family protein Des1 in *Arabidopsis*. *Int. J. Mol. Sci.* 2021; **22**, 4738.
- [9] H Seok, LV Nguyen, H Park, VN Tarte, J Ha, S Lee and Y Moon. *Arabidopsis* non-TZF gene *AtC3H17* functions as a positive regulator in salt stress response. *Biochem. Biophys. Res. Comm.* 2018; **498**, 954-9.
- [10] S Bogamuwa and JC Jang. Plant tandem CCCH zinc finger proteins interact with ABA, drought, and stress response regulators in processing-bodies and stress granules. *PLoS One* 2016; **11**, e0151574.
- [11] KK Vinod, JR Meenattoor, PM Priyadarshan, J Pothen, D Chaudhuri, AK Krishnakumar, MR Sethuraj and SN Potty. Early performance of some clones of *Hevea brasiliensis* in Tripura. *Indian J. Nat. Rubber Res.* 1996; **9**, 123-9.
- [12] Y Zhang, J Leclercq and P Montoro. Reactive oxygen species in *Hevea brasiliensis* latex and relevance to tapping panel dryness. *Tree Physiol.* 2016; **37**, 261-9.

- [13] P Suwanmanee, N Sirinupong and W Suvachittanont. *Regulation of 3-hydroxy-3-methylglutaryl-CoA synthase and 3-hydroxy-3-methylglutaryl-CoA reductase and rubber biosynthesis of Hevea brasiliensis (B.H.K.) Mull. Arg. In: TJ Bach and M Rohmer (Eds.). Isoprenoid synthesis in plants and microorganism. Springer, New York, 2013, p. 315-27.*
- [14] P Suwanmanee, S chocknukul, N Sirinupong, T Phattamanont, C Chantrapradist and P Jewtragoon. Selection of gene marker for identification of high latex yielding Hevea clone. *In: Proceedings of the 19<sup>th</sup> Thaksin University annual conference, Songkhla, Thailand. 2009, p. 304-11.*
- [15] E Gasteiger, C Hoogland, A Gattiker, S Duvaud, MR Wilkins, RD Appel and A Bairoch. *Protein identification and analysis tools on the ExPASy server. In: JM Walker (Ed.). The proteomics protocols handbook. Humana Press, New Jersey, 2005, p. 571-607.*
- [16] TA Hall. Bioedit: A user-friendly biological sequence alignment editor analysis program for windows 95/98/NT. *Nucleic Acids Symp.* 1999; **41**, 95-8.
- [17] K Tamura, G Stecher and S Kumar. MEGA11: Molecular evolutionary genetic analysis version 11. *Mol. Biol. Evol.* 2021; **38**, 3022-7.
- [18] I Lectunic, S Khedka and P Bork. SMART: Recent updates, new developments, and status in 2020. *Nucleic Acids Res.* 2021; **49**, 458-60.
- [19] GE Crooke, G Hon, JM Chandonia and SE Brenner. WebLogo: A sequence logo generator. *Genome Res.* 2004; **14**, 1188-90.
- [20] W Liu, Y Xie, J Ma, X Luo, P Nie, Z Zuo, U Lahrmann, Q Zhao, Y Zheng, Y Zhao, Y Xue and R Ren. IBS: An illustrator for the presentation and visualization of biological sequences. *Bioinformatics* 2015; **31**, 3359-61.
- [21] S Kosuki, M Hasebe, M Tomita and H Yanagawa. Systematic identification of yeast cell cycle-dependent nucleocytoplasmic shutting protein by prediction of composite motifs. *Proc. Natl. Acad. Sci. Unit. States Am.* 2009; **106**, 10171-6.
- [22] W Zheng, W Zhang, Y Li, R Pearce and EW Bell. Folding non-homology proteins by coupling deep-learning contact map with I-TASSER assembly simulations. *Cell Rep. Meth.* 2021; **1**, 100014.
- [23] WL Delano, The PyMOL molecular graphics system, Available at: <http://www.Pymol.org>, accessed January 2022.
- [24] VB Chen, WB Arendall, JJ Headd, DA Keedy, RM Immormino, GJ Kapral, LW Murray, JS Richardson and DC Richardson. MolProbity: All-atom structure validation for macromolecular crystallography. *Acta Crystallogr. D Biol. Crystallogr.* 2010; **66**, 12-21.
- [25] Z Xie, W Lin, G Yu, Q Cheng, B Xu and B Huang. Improved cold tolerance in switchgrass by a novel CCCH-type zinc finger transcription factor gene, PvC3H72, associated with ICE1-CBF-COR regulation and ABA-responsive genes. *Biotechnol. Biofuels* 2019; **12**, 224.
- [26] J Sun, H Jiang, Y Xu, H Li, X Wu and C Li. The CCCH-type zinc finger proteins *AtSZF1* and *AtSZF2* regulate salt stress response in *Arabidopsis*. *Plant Cell Physiol.* 2007; **48**, 1148-58.
- [27] MC Pomeranz, C Hah, P Lin, SG Kang, JJ Finer, PJ Blackshear and JC Jang. The *Arabidopsis* tandem zinc finger protein *AtTZF1* traffics between the nucleus and cytoplasmic foci and binds both DNA and RNA. *Plant Physiol.* 2010; **152**, 151-65.
- [28] ZJ Lorkovic and A Barta. Genome analysis: RNA recognition motif (RRM) and K homology (KH) domain RNA binding proteins from the flowering plant *Arabidopsis thaliana*. *Nucleic Acids Res.* 2002; **30**, 623-35.
- [29] MH Rider, L Bertrand, D Vertommen, PA Michels, GG Rousseau and L Hue. 6-phosphofructo-2-kinase/fructose-2,6-bisphosphatase: head-to-head with a bifunctional enzyme that controls glycolysis. *Biochem. J.* 2004; **381**, 561-78.
- [30] EB Tikhonova, AS Ethayathulla, Y Su, P Harharan, S Xie and L Guan. A transcription blocker isolated from a designed repeat protein combinatorial library by *in vivo* functional screen. *Sci. Rep.* 2014; **5**, 8070.
- [31] C Mi, L Zhang, G Huang, G Shao, F Yang, X You, MQ Dong, S Sun and SF Sui. Structural basis for assembly of TRAPP II complex and specific activation of GTPase Ypt31/32. *Sci. Adv.* 2022; **8**, eabi5603.
- [32] P Barraud, S Banerjee, WI Mohamed, MF Jantsh and FHT Allain. A bimodular nuclear localization signal assembled via an extended double-strand RNA-binding domain acts as an RNA sensing signal for transpotin1. *Proc. Natl. Acad. Sci. Unit. States Am.* 2014; **111**, E1853-E1861.
- [33] B Pi, J Pan, M Xio, X Hu, L Zhang, M Chen, B Liu, Y Ruan and Y Huang. Systematic analysis of CCCH zinc finger family in *Brasica napus* showed that *BnRR-TZFs* are involved in stress resistance. *BMC Plant Biol.* 2021; **21**, 555.

- [34] S Xin, Y Hua, J Li, X Dai, X Yang, J Udayabhanu, H Huang and T Huang. Comparative analysis of latex transcriptomes reveals the potential mechanisms underlying rubber molecular weight variations between the *Hevea brasiliensis* clones RRIM600 and Reyan 7-33-97. *BMC Plant Biol.* 2021; **21**, 244.
- [35] D Li, L Hao, H Liu, M Zhao, Z Deng, Y Li, R Zeng and W Tian. Next-generation sequencing, assembly, and comparative analyses of the latex transcriptomes from two elite *Hevea brasiliensis* varieties. *Tree Genet. Genomes* 2015; **11**, 98.
- [36] J Santos, LE Oliveira, VT Coelho, G Lopes, T Souza, AC Porto, J Lira, R Massote, C Rocha and MP Gomes. Performance of *Hevea brasiliensis* under drought conditions on osmoregulation and antioxidant activity through evaluation of vacuolar invertase and reducing sugars. *Plant Sci. Today* 2021; **8**, 312-23.
- [37] TP Liu, YF Zhuang, XL Guo and YJ Li. Molecular mechanism of ethylene stimulation of latex yield in rubber tree (*Hevea brasiliensis*) revealed by *de novo* sequencing and transcriptome analysis. *BMC Genom.* 2016; **17**, 257.
- [38] B Pi, X He, HY Ruan, JC Jang and Y Huang. Genome-wide analysis and stress-responsive expression of CCCH zinc finger family genes in *Brassica rapa*. *BMC Plant Biol.* 2018; **18**, 373.
- [39] N Chevalier, L Bertrand, MH Rider, FR Opperdoes, DJ Ringden and PAM Michels. 6-phosphofructo-2-kinase and fructose-2,6-bisphosphatase in Trypanosomatidae. *FEBS J.* 2005; **272**, 3542-60.
- [40] T Banzai, N Hanagata, Z Dubinsky and I Karube. Fructose-2,6-bisphosphate contents were increased in response to salt, water, and osmotic stress in leaves of *Bruguiera gymnorhiza* by differential changes in the activity of the bifunctional enzyme 6-phosphofructo-2-kinase/fructose-2,6-bisphosphate 2 phosphatase. *Plant Mol. Biol.* 2003; **53**, 51-9.
- [41] TH Nielson, JH Ruang and D Villadson. Fructose-2,6-bisphosphate: A traffic signal in plant metabolism. *Trends Plant Sci.* 2004; **9**, 557-63.
- [42] X Guo and K Chong. Cold signalling in plants: Insights into mechanisms and regulation. *J. Integr. Plant Biol.* 2018; **60**, 745-56.
- [43] R Bagur and G Hajnóczky. Intracellular Ca<sup>2+</sup> sensing: Role in calcium homeostasis and signaling. *Mol. Cell* 2017; **66**, 780-8.
- [44] Y Aoki, S Takahashi, D Takayama, Y Ogata, N Sakurai, H Suzuki, K Assawatreeeratanakul, D Wititsuwannakul, R Wititsuwannakul, D Shibata, T Koyama and T Nakayama. Identification of laticifer-specific genes and their promoter regions from a natural rubber producing plant *Hevea brasiliensis*. *Plant Sci.* 2014; **225**, 1-8.